Tetrahedron Letters 51 (2010) 1545–1549

Contents lists available at ScienceDirect

Tetrahedron Letters

journal homepage: www.elsevier.com/locate/tetlet

Analytical investigations of the behavior of silole-core dendrimers with peripheral globotriaose in water and acetone/water mixed solvent

Hiroaki Aizawa *, Ken Hatano, Hitoshi Saeki, Nobuaki Honsho, Tetsuo Koyama, Koji Matsuoka, Daiyo Terunuma

Division of Material Science, Graduate School of Science and Technology, Saitama University, 255 Shimo-Ohkubo, Sakura-ku, Saitama 338-8570, Japan

ARTICLE INFO

Article history:
Received 7 November 2009
Revised 15 December 2009
Accepted 12 January 2010
Available online 18 January 2010

ABSTRACT

A new compound having a 2,3,4,5-tetraphenylsilole derivative on the center silicon of Dumbbell(1)6Gb3; Silole-Dumbbell(1)6Gb3 (**1**) was previously reported. It was found that **1** exhibited strongly increased fluorescence both in water and in a 96% acetone/water mixed solvent. The physical behavior of **1** in water and in the 96% acetone/water mixed solvent was investigated, and analyses including fluorescence quantum yields, dynamic-light-scattering (DLS), atomic-force-microscopy (AFM), and fluorescence microscopy were carried out. It was clarified that **1** dynamically formed different types of aggregates in water and in higher acetone concentrations to yield high aggregation-induced emission (AIE) effects due to the formation of micelle-like particles in water and inversion-type micelles in the acetone/water mixed solvent, respectively.

A series of new glycoclusters, carbosilane dendrimers carrying periphery globotriaose (Gb3; Galα1-4Gαlb1-4Glcβ1-), known to have a selective affinity to Shiga toxins (Stxs; Stx1 and Stx2) produced by *Escherichia coil* O157:H7, were previously prepared.[1a–c] The bioactive evaluation of the new glycoclusters demonstrated that only Dumbbell(1)6Gb3 and Dumbbell(2)18Gb3 were highly effective among the carbosilane dendrimers having periphery globotriaose for neutralizing Stxs both in vivo and in vitro. This was the first example of successful neutralization of Stxs in vivo. These results showed that for effective inhibition of Stxs, it is important to appropriately design the number of saccharides and the formula for the carbosilane dendrimers.[2a–d] Subsequently, it was demonstrated that the Dumbbell(1)6-type compounds having other saccharides such as sialyllactose[3a,3b] and lacto-*N*-neotetraose[4] were also very effective for inhibiting the influenza virus and the dengue virus, respectively.

On the other hand, siloles show unique enhanced fluorescence in a poor solvent, which is known as aggregation-induced emission (AIE).[5] Tang and co-workers reported[6a–d] that the fluorescence intensity of siloles increased remarkably above a ratio of 50% water for the addition of a portion of water to a solvent of a hydrophobic silole derivative in ethanol. It is considered that the AIE effects are generated by restricting the rotation of the substituted phenyl groups on the silole by aggregation.[7]

As described in a previous Letter, Silole-Dumbbell(1)6Gb3(**1**) (Fig. 1) having a 2,3,4,5-tetraphenylsilole derivative on the center silicon of Dumbbell(1)6Gb3 was designed and successfully prepared.[8] Interestingly, it was found that **1** exhibited strongly increased fluorescence intensity at 475 nm by 360 nm excitation, both in water and in acetone/water mixed solvents with over 80% acetone. An application of this for fluorescence detection for viruses was investigated using the specific character of **1** such as the enhanced glycocluster effects and AIE effects by aggregation in water as described in the literature.[9] In the present study, instrument-based analyses, including fluorescence quantum yields, dynamic-light-scattering (DLS), atomic-force-microscopy (AFM), and fluorescence microscopy, were conducted in order to elucidate the detailed behavior of **1** in water and in acetone/water mixed solvent.

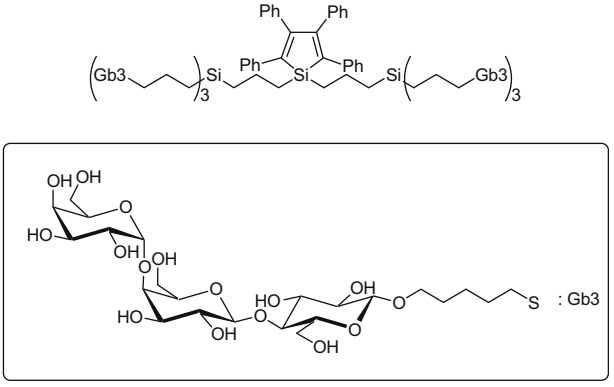

Figure 1. Structure of **1**.

* Corresponding author.
E-mail address: aiai0922@gmail.com (H. Aizawa).

0040-4039/$ - see front matter Crown Copyright © 2010 Published by Elsevier Ltd. All rights reserved.
doi:10.1016/j.tetlet.2010.01.041

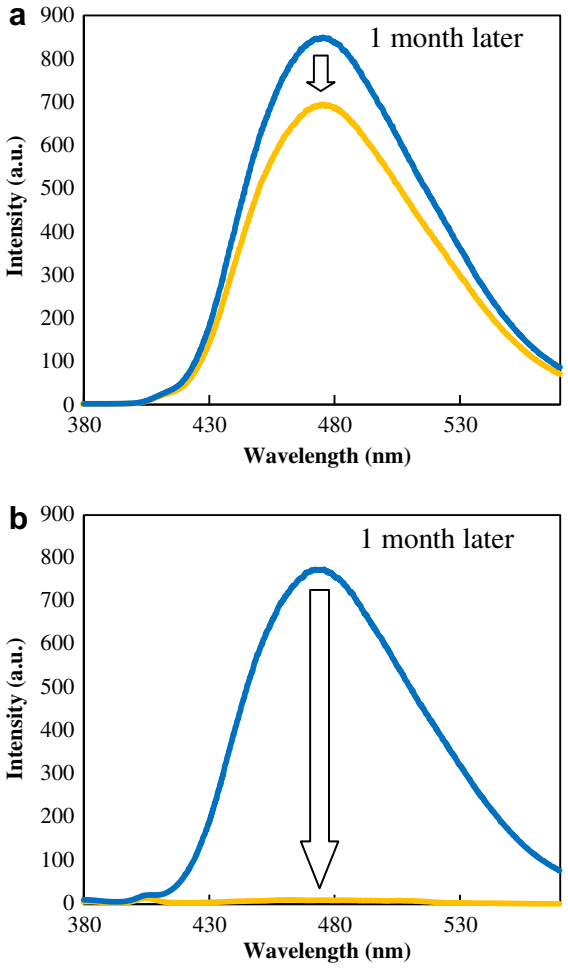

Figure 2. Time-dependent changes of PL spectra of **1**, (a) in water, (b) in 96% acetone/water mixed solvent. Concn: 1.0 μM; Ex.: 360 nm.

To the best of our knowledge, all the siloles that show AIE effects are hydrophobic and are soluble in common organic solvents such as acetone and alcohol. In these siloles, AIE effects appeared by adding a portion of water to the silole in an acetone or alcohol solution. In contrast, **1** is soluble in water and not soluble in ordinary polar organic solvents, such as acetone and methanol. In a previous Letter, the relationship between the fluorescence intensities of **1** and the ratio of the mixed solvents of acetone and water were described.[5] Interestingly, **1** exhibited similar AIE effects both in water and in a 96% acetone/water

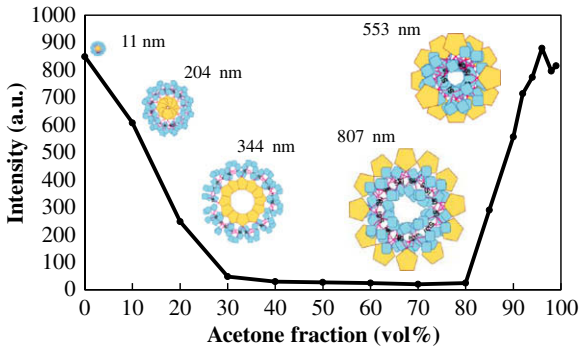

Figure 3. Correlation between PL intensity and aggregation-shape images of **1** in various proportion of acetone/water mixed solvent.

Table 1
PL intensity, Φ_{PL} and particle size of **1** in various proportion of acetone/water mixed solvent

Mixed proportion acetone/water	PL intensity[a]	Φ_{PL}[b]	Particle size[b] (nm)
0/100	849.2	0.70	11
10/90	608.3	0.49	208
20/80	248.6	0.24	340
50/50	27.1	0.03	—[c]
85/15	290.9	0.13	800
90/10	557.7	0.33	550

[a] Concn: 1.0 μM, Ex.: 360 nm, Em.: 475 nm.
[b] Concn: 2.3 μM.
[c] Not detected.

mixed solvent. However, the solution of **1** in water and in the 96% acetone/water mixed solvent showed quite different stabilities. It maintained almost the same fluorescence after one month in water, but the fluorescence dramatically decreased in the 96% acetone/water mixed solvent, which may be due to the precipitation of **1** (Fig. 2).

It is of interest to investigate the detailed behavior of **1** in water and acetone/water mixed solvent to reveal the reason why **1** shows high fluorescence both in water and in the acetone in water mixed solvents. First, quantum yields of **1** were determined in water and in the acetone/water mixed solvent. Quantum yields were measured at 10 μM of **1** using quantum yield measurement equipment, the Hamamatsu photonics C9920-02 (Fig. 3). The quantum yield was 0.70 in water. With increasing acetone concentration up to 60%, the fluorescence intensity gradually decreased; the quantum yield decreased to 0.03 at 50% acetone/water mixed solvent (Table 1). Although, the fluorescence intensity barely changed up to 80% acetone, it began to increase again with increasing acetone content above 80%, and the quantum yield increased up to 0.33 for the 90% acetone/water mixed solvent. These results show that the fluorescence intensity and the quantum yields are directly correlated, depending on the solvent used.

On the other hand, it is already known that the quantum yield of the film prepared from 1,1-dimethyltetraphenylsilole is 0.76 and that of a solution in cyclohexane is 0.0022.[10] Based on the quantum yields for **1** (Φ_{PL} 0.70) obtained here, it is considered that silole moieties of **1** in water form rigid aggregates as well as the film. Because the quantum yield of **1** is significantly higher than that in the 50% acetone/water in which **1** is homogeneously dissolved (Φ_{PL} 0.03). In contrast, **1** forms soft aggregates in the 90% acetone/water mixed solvent (Φ_{PL} 0.33). The quantum yield of **1** in less than 5% concentration of water could not be obtained accurately, because of rapid precipitation of **1** in the solvent.

Next, DLS measurements of **1** in water and in mixed solvent of water and acetone were demonstrated using a dynamic laser scattering instrument, Nikkiso UPA-UT (Fig. 4). Particle sizes in the corresponding mixed solvents were measured by DLS for a concentration of **1** of 1 mg per 100 ml (2.3 μM) (Fig. 4a). The corresponding particle sizes in water, 10% and 20% acetone/water mixed solvent were observed to be around 11, 208 and 340 nm, respectively. In contrast, when acetone concentrations were enriched up to 85% and 90%, the particle sizes were decreased from 800 nm to 550 nm, respectively (Fig. 4b). Interestingly, it was found that increasing the concentration of acetone up to 20% enlarged the particle size and gave a wider distribution.

These results suggest a picture wherein particles of **1** in water and in water containing acetone up to 20% form aggregates with oriented hydrophobic silole having a carbosilane dendrimer inside and hydrophilic Gb3 outside, similar to a micelle. In contrast, those in water containing over 30% acetone form aggregates with oriented silole having carbosilane dendrimer outside and Gb3 inside, similar to a reversed micelle. It would also be rational to

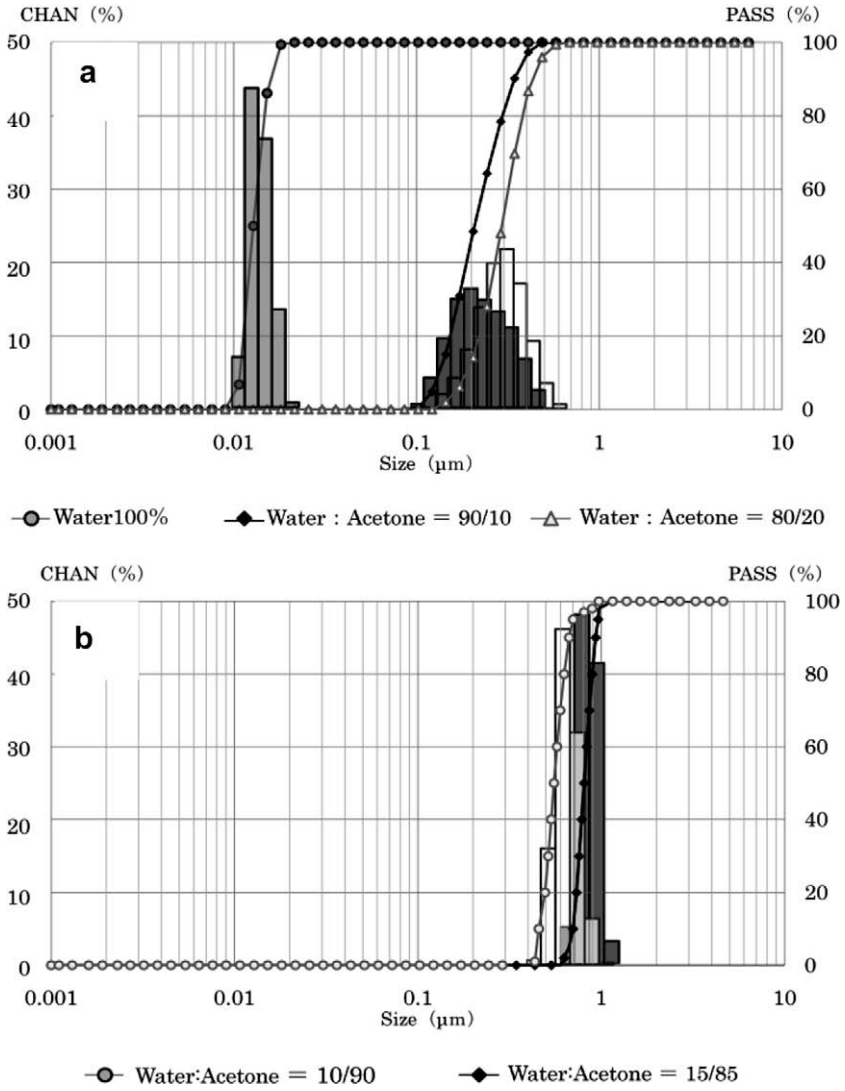

Figure 4. Particle size of **1** in various proportion of acetone/water mixed solvent. (a) in water and 10%, 20% acetone/water mixed solvent, (b) 85% and 90% acetone/water mixed solvent. Concn: 2.3 μM.

consider that in the presence of a small amount of acetone, hydrophobic acetone penetrates into the silole having the carbosilane dendrimer to enlarge the particle size, based on the proportion of acetone in water up to 20%. It is known that the depression of rotation of the phenyl group on siloles increases fluorescence and quantum yield of the silole by the AIE effect. So it is possible to relate the enlargement of the particle size with increasing acetone concentration up to 20% in water, making the aggregates less dense to yield lower fluorescence and quantum yields. In contrast, with increasing acetone concentration above 80%, the aggregates form higher density, to give increased fluorescence and quantum yields. In preliminary experiments, Silole-Dumbbell(1)6 carrying a common hydrophilic function on the periphery, such as quaternary ammonium salts or sodium carboxylates, was prepared, and the AIE effects were investigated by following the procedures described above. However, no analogous phenomenon was found. These results reveal that the balance of a hydrophobic group and a hydrophilic group is essential in order to demonstrate these unique AIE effects as described for **1**.

AFM measurements of **1** at 45 μM in water and in acetone/water mixed solvent were also carried out (Fig. 5). The samples for AFM analysis were prepared by dropping a portion of the solution on a mica surface pretreated with 3-aminopropyltriethoxysilane. Three-dimensional (3D) AFM analysis in water revealed the existence of relatively small particles (Fig. 5a). Cross-sectional analysis showed that the aggregates sunk on the mica surface had a sharp particle diameter (5c) around 11 nm (Fig. 5b and c). Particle sizes measured by AFM analysis in water were consistent with those obtained by DLS analysis in water. For AFM characterization and cross-sectional analysis in a 50% acetone/water mixed solvent, a few particles under 4 nm in diameter, which possibly aggregated during the drying of the sample and a relatively flat surface on the mica base were observed (Fig. 5d–f). Unfortunately, acetone was too volatile to obtain an AFM image in 98% acetone/water mixed solvent. The sample was dried at room temperature. AFM measurement of the dried sample showed a large lump of coexisting precipitates with over 300 nm height and crater-like dents (Fig. 5g–i).

The samples prepared in water and in 50% acetone/water mixed solvent were dried at room temperature. Observations using fluorescence microscopy for three dried samples, including those dried from 98% acetone/water mixed solvent, were carried out (Fig. 6). For fluorescence microscope images, taken under conditions of excitation wavelength of 350/50 nm, the observed wavelength was 420 nm at a 100× magnification. Surprisingly, the aggregates formed in the solutions were sufficiently stable to be observed

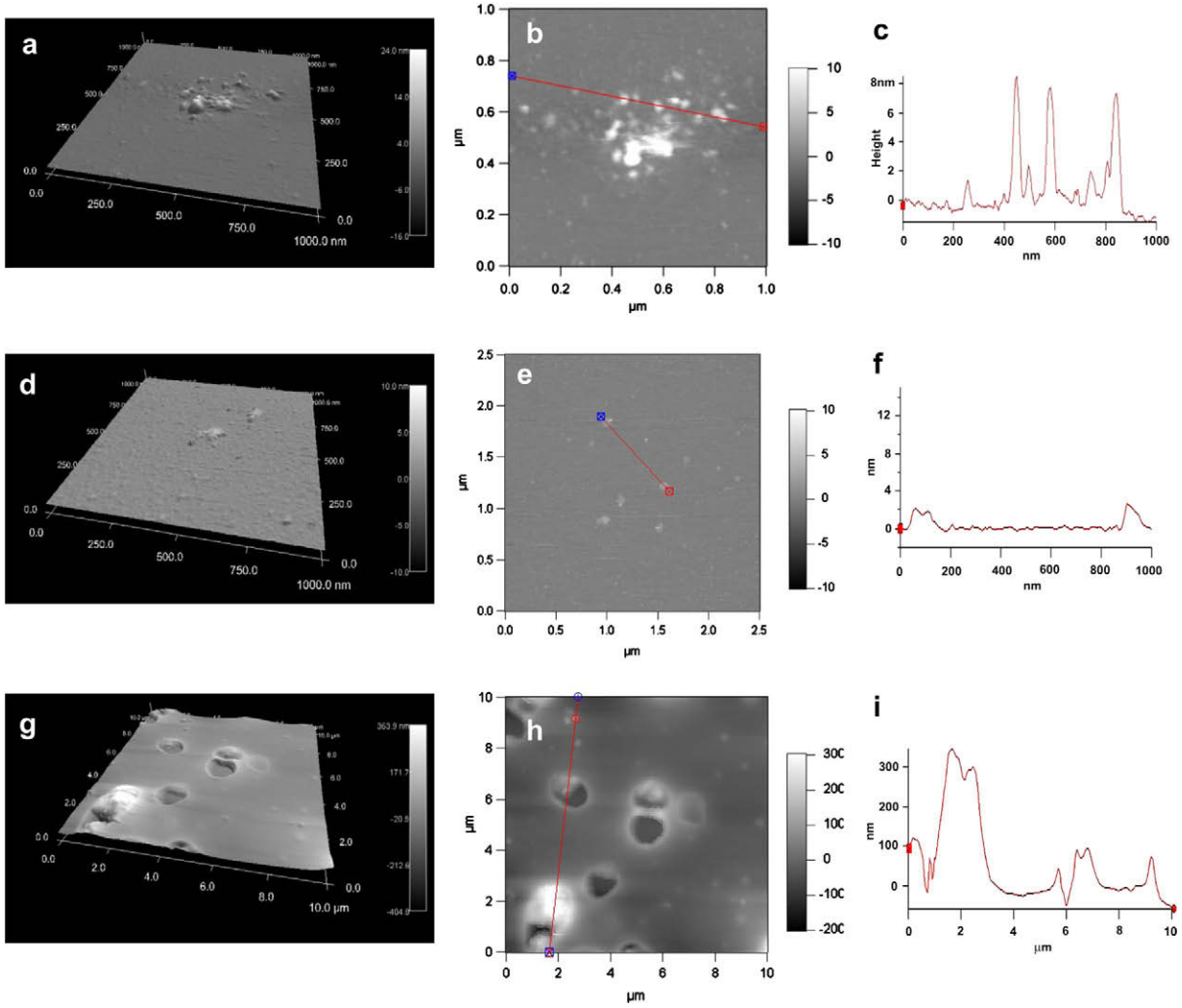

Figure 5. 3D AFM images (left, panel a, d, g) and plan view AFM images (center, panel b, e, h) and cross section AFM images (right, panel c, f, i) of **1** on mica at various conditions**.** AFM images in water measured by AC mode (top). AFM images in 50% acetone/water mixed solvent measured by AC mode (middle). AFM images measured under dry condition, the sample prepared from **1** in 96% acetone/water mixed solvent (bottom).

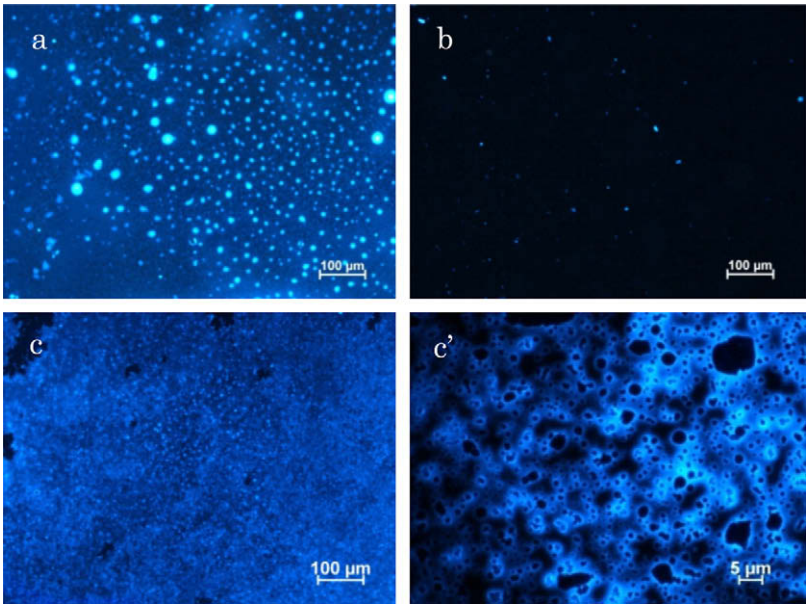

Figure 6. Fluorescence microscope images of dry samples of **1** prepared from (a) water, (b) 50% acetone/water mixed solvent, (c) and (c′) 98% acetone/water mixed solvent.

directly even on the dried samples. In the sample prepared from the water solution, there were many pale and small spherical particles on the mica surface (Fig. 6a), and no strongly fluorescent particles were found and only a black wide plane was observed in the sample of 50% acetone/water mixed solvent (Fig. 6b). In contrast, the fluorescence microscope image obtained for the sample of 98% acetone/water mixed solvent displayed a different picture (Fig. 6c). This was more clearly observed in the micrograph using 1000X magnification (Fig. 6c′). A number of circle-like fluorescence patterns with different sizes, and one circle-like fluorescence lie around a small black circle. Thus, it was confirmed that the particles produced in the solutions were sufficiently stable to be kept even under dry conditions.

It was concluded, based on DLS, AFM, and fluorescence microscopy observations, that **1** forms water-soluble, small micelle-like spherical particles with hydrophobic siloles for the inside direction to yield higher density of siloles with hydrophilic Gb3 outside in the water solution. **1** also forms an inverse particle with low solubility in 98% acetone/water mixed solvent to give enhanced fluorescence and high quantum yield by the AIE effect.

Acknowledgments

The authors are grateful to Professor Kohei Tamao, Dr. Tsukasa Matsuo, and Dr. Katsunori Suzuki of Advanced Science Institute (RIKEN) for measuring fluorescence quantum yield. The authors thank Assistant Professor Norihito Sogoshi of Saitama University for determination for a part of DLS analysis.

Supplementary data

Supplementary data associated with this article can be found, in the online version, at doi:10.1016/j.tetlet.2010.01.041.

References and notes

1. (a) Matsuoka, K.; Kurosawa, H.; Esumi, Y.; Terunuma, D.; Kuzuhara, H. *Carbohydr. Res.* **2000**, *329*, 765–772; (b) Nishikawa, K.; Matsuoka, K.; Kita, E.; Okabe, N.; Mizuguchi, M.; Hino, K.; Miyazawa, S.; Yamasaki, C.; Aoki, J.; Takashima, S.; Yamakawa, Y.; Nishijima, M.; Terunuma, D.; Kuzuhara, H.; Natori, Y. *Proc. Natl. Acad. Sci. U.S.A.* **2002**, *99*, 7669–7674; (c) Miura, Y.; Sasao, Y.; Dohi, H.; Nishida, Y.; Kobayashi, K. *Anal. Biochem.* **2002**, *310*, 27–35.
2. (a) Watanabe, M.; Matsuoka, K.; Kita, E.; Igai, K.; Higashi, N.; Miyagawa, A.; Watanabe, T.; Yanoshita, R.; Samejima, Y.; Terunuma, D.; Natori, Y.; Nishikawa, K. *J. Infect. Dis.* **2004**, *189*, 360–368; (b) Yamada, A.; Hatano, K.; Matsuoka, K.; Koyama, T.; Esumi, Y.; Koshino, H.; Hino, K.; Nishikawa, K.; Natori, Y.; Terunuma, D. *Tetrahedron* **2006**, *62*, 5074–5083; (c) Watanabe, M.; Igai, K.; Matsuoka, K.; Miyagawa, A.; Watanabe, T.; Yanoshita, R.; Samejima, Y.; Terunuma, D.; Natori, Y.; Nishikawa, K. *Infect. Immun.* **2006**, *74*, 1984–1988; (d) Nishikawa, K.; Watanabe, M.; Kita, E.; Igai, K.; Omata, K.; Yaffe, M.; Natori, Y. *FASEB J.* **2006**, *20*, 2597.
3. (a) Matsuoka, K.; Oka, H.; Koyama, T.; Esumi, Y.; Terunuma, D. *Tetrahedron Lett.* **2001**, *42*, 3327–3330; (b) Oka, H.; Onaga, T.; Koyama, T.; Guo, C.-T.; Suzuki, Y.; Esumi, Y.; Hatano, K.; Terunuma, D.; Matsuoka, K. *Bioorg. Med. Chem. Lett.* **2008**, *18*, 4405–4408.
4. Yamada, A.; Hatano, K.; Koyama, T.; Matsuoka, K.; Esumi, Y.; Terunuma, D. *Carbohydr. Res.* **2006**, *341*, 467–473.
5. Luo, J.; Xie, Z.; Lam, J. W. Y.; Cheng, L.; Tang, B. Z.; Chen, H.; Qiu, C.; Kwok, H. S.; Zhan, X.; Liu, Y.; Zhu, D. *Chem. Commun.* **2001**, 1740–1741.
6. (a) Chen, J.; Law, C. C. W.; Lam, J. W. Y.; Dong, Y.; Lo, S. M. F.; Williams, I. D.; Zhu, D.; Tang, B. Z. *Chem. Mater.* **2003**, *15*, 1535–1546; (b) Zeng, Q.; Li, Z.; Dong, Y.; Di, C.; Qin, A.; Hong, Y.; Ji, L.; Zhu, Z.; Jim, C. K. W.; Yu, G.; Li, Q.; Li, Z.; Liu, Y.; Qin, J.; Tang, B. Z. *Chem. Commun.* **2007**, 70–72; (c) Liu, J.; Lam, J.; Tang, B. Z. *J. Inorg. Organomet. Polym. Mater.* **2009**, *19*, 249–285; (d) Hong, Y.; Lam, J.; Tang, B. Z. *Chem. Commun.* **2009**, *2009*, 4332–4353.
7. Li, Z.; Dong, Y.; Mi, B.; Tang, Y.; Haussler, M.; Tong, H.; Dong, Y.; Lam, J. W. Y.; Ren, Y.; Sung, H. H. Y.; Wong, K. S.; Gao, P.; Williams, I. D.; Kwok, H. S.; Tang, B. Z. *J. phys. chem. B* **2005**, *109*, 10061–10066.
8. Hatano, K.; Aizawa, H.; Yokota, H.; Yamada, A.; Esumi, Y.; Koshino, H.; Koyama, T.; Matsuoka, K.; Terunuma, D. *Tetrahedron Lett.* **2007**, *48*, 4365–4368.
9. Hatano, K.; Saeki, H.; Yokota, H.; Aizawa, H.; Koyama, T.; Matsuoka, K.; Terunuma, D. *Tetrahedron Lett.* **2009**, *50*, 5816–5819.
10. Yu, G.; Yin, S.; Liu, Y.; Chen, J.; Xu, X.; Sun, X.; Ma, D.; Zhan, X.; Peng, Q.; Shuai, Z.; Tang, B.; Zhu, D.; Fang, W.; Luo, Y. *J. Am. Chem. Soc.* **2005**, *127*, 6335–6346.